Chemosphere 181 (2017) 241–249

Contents lists available at ScienceDirect

Chemosphere

journal homepage: www.elsevier.com/locate/chemosphere

Nanostructural and mechanical property changes to spider silk as a consequence of insecticide exposure

Marco Benamú [a, b], Mariángeles Lacava [a, b], Luis F. García [c], Martín Santana [b], Jian Fang [d], Xungai Wang [d], Sean J. Blamires [e, *]

[a] Centro Universitario de Rivera (Universidad de la República), Rivera, Uruguay
[b] Laboratorio Ecología del Comportamiento (Instituto de Investigaciones Biológicas Clemente Estable), Montevideo, Uruguay
[c] Centro Universitario Regional del Este (Universidad de la República) Treinta y Tres, Uruguay
[d] Institute for Frontier Materials (IFM), Deakin University, Waurn Ponds Campus, Geelong, Vic 3220, Australia
[e] Evolution & Ecology Research Centre, School of Biological, Earth & Environmental Sciences, The University of New South Wales, Sydney NSW 2052, Australia

HIGHLIGHTS

- Spiders are beneficial organisms on arable lands that insecticides affect adversely.
- We performed mechanical and nanostructural analyses on exposed spider silks.
- The insecticides affected spider silk mechanics, nanostructures and composition.
- The effects on silk and webs render the insecticides detrimental to spiders.

ARTICLE INFO

Article history:
Received 16 January 2017
Received in revised form
27 March 2017
Accepted 17 April 2017
Available online 21 April 2017

Handling Editor: A. Gies

Keywords:
Parawixia audax
Broad spectrum foliar insecticide
X-ray scattering
Silk nanostructures
Silk mechanics
Spidroin expression
Orb web spiders

ABSTRACT

Neonicotinoids are one of the world's most extensively used insecticides, but their sub-lethal influences on non-target and beneficial organisms are not well known. Here we exposed the orb web spider *Parawixia audax*, which is found on arable lands in Uruguay, to a sub-lethal concentration of the broad spectrum insecticide Geonex (thiamethoxam + lambda-cyhalothrin) and monitored their web building. We collected their major ampullate silk and subjected it to tensile tests, wide-angle X-ray diffraction (WAXS) analysis, and amino acid composition analysis. Around half of the exposed spiders failed to build webs. Those that built webs produced irregular webs lacking spiral threads. The mechanical properties, nanostructures, and amino acid compositions of the silk were all significantly affected when the spiders were exposed to insecticides. We found that silk proline, glutamine, alanine and glycine compositions differed between treatments, indicating that insecticide exposure induced downregulation of the silk protein MaSp2. The spiders in the control group had stronger, tougher and more extensible silks than those in the insecticide exposed group. Our WAXS analyses showed the amorphous region nanostructures became misaligned in insecticide exposed silks, explaining their greater stiffness. While the insecticide dose we subjected *P. audax* to was evidently sub-lethal, the changes in silk physicochemical properties and the impairment to web building will indelibly affect their ability to catch prey.

1. Introduction

Neonicotinoids and pyrethroids are broad spectrum, biodegradable, neurotoxic insecticides that are effective at eliminating insect pests such as aphids, whiteflies, plant-hoppers and thrips from arable lands (Asquith and Hull, 1973; Honda et al., 2006; Ishaaya et al., 2007; Elbert et al., 2008). Compared to many other insecticides these are less toxic to birds and mammals than insects (Tomizawa and Casida, 2005). Compounds such as imidacloprid, acetamiprid and thiamethoxam act by disrupting insect nicotinic acetylcholine receptor synaptic transmission within invertebrate central nervous systems (Tomizawa et al., 1995; Jones and Sattelle, 2010). Accordingly they adversely affect insect cognition, learning,

* Corresponding author.
E-mail address: s.blamires@unsw.edu.au (S.J. Blamires).

http://dx.doi.org/10.1016/j.chemosphere.2017.04.079
0045-6535/

orientation, decision making and feeding (Tomizawa et al., 1995). Due to their broad spectrum of efficacy and distinct mode of action, neonicotinoid and pyrethroid use by agriculturalists is expanding worldwide (Honda et al., 2006; Dai et al., 2010). In Uruguay use of these insecticides has increased exponentially of late due to the recent arrival of new crops, such as soybean (Ministry of Agriculture and Fisheries of Uruguay, 2013; Benamú et al., 2013; Lacava, 2014).

While neonicotinoids, pyrethroids and other insecticides effectively decrease pest populations in the short term, their continuous use may induce secondary environmental damage, loss of biodiversity, and interrupt ecological processes. Furthermore, they can negatively affect non-target invertebrates, including pollinators and the natural enemies of crop pests (Pisa et al., 2015; Michalko and Kosulic, 2016). Spiders, for instance, can be negatively affected by insecticide applications (Benamú, 1999; Sunderland, 1999; Landis et al., 2000; Symondson et al., 2002; Hoefler et al., 2006; Öberg et al., 2007). In addition to direct lethal effects (Pekar, 2013; Michalko and Kosulic, 2016), insecticides have sub-lethal effects on spiders, including various developmental, biochemical, physiological, and behavioural impairments (Landis et al., 2000; Symondson et al., 2002; Desneux et al., 2007; Benamú et al., 2007, 2013; Benamú, 2010; Pekar, 2013; Royaute et al., 2015).

All spiders secrete silk (Breslauer and Kaplan, 2012). Orb web spiders (Orbiculariae) have the most impressive silk toolkits, secreting up to seven types of silk (major and minor ampullate, tubuliform, aciniform, pyriform, aggregate and flagelliform silks) from specialized glands (Blackledge and Hayashi, 2006; Heim et al., 2009; Blamires et al., 2017). These silks may combine to perform specific functions as a component of the prey-catching web or as components of eggsac cocoons (Blamires et al., 2017). Of these silks, major ampullate silk (MAS), the silk comprising the supporting frame and radial treads of orb webs, has the most impressive properties, with a strength and toughness exceeding most high performing synthetic materials, even Kevlar® (Vollrath et al., 2013; Blamires et al., 2017).

MAS is hierarchically organized with a lipid and glycoprotein-rich skin layer covering a fibrous outer- and inner-core (Papadopoulos et al., 2009; Heim et al., 2010; Blamires et al., 2017). The core is composed of two types of proteins (conventionally called spidroins); MaSp1 (derived from Major ampullate Spidroin 1) and MaSp2 (Major ampullate Spidroin 2). These proteins arrange as ordered crystalline regions dispersed among disordered semi-crystalline and amorphous regions. The crystalline regions contain stacked pleated β−sheet nanostructures while the semi-crystalline and amorphous regions arrange as matrices of 3_{10}-helices, β-turns or β −spirals nanostructures depending on the amino acid composition of the silk (Jelinski, 1998; Sponner et al., 2007; Jenkins et al., 2013; Blamires et al., 2016).

MAS is secreted from the major ampullate gland, which consists of a tail, sac and duct region (Andersson et al., 2013; Rising and Johansson, 2015; Blamires et al., 2017). The spidroins are secreted into the tail of the major ampullate gland and stored in the sac as a solution called dope (Heim et al., 2009; Vollrath et al., 2013). The dope flows into the duct where biophysical actions induce the silk proteins to form the different nanostructures (Hagn et al., 2011; Schwarze et al., 2013). Unfortunately the energetic, enzymatic or other biochemical processes facilitating protein nanostructural formation are not well known. However, we know that the nanostructures and the subsequent mechanical properties of MAS are sensitive to variations in temperature and the spider's diet (Craig et al., 2000; Tso et al., 2005; Blamires et al., 2015), thus suggesting nanostructure formation is a metabolically costly process.

Here we performed an experiment exposing the South American orb web spider *Parawixia audax* (Araneae, Araneidae) to a sub-lethal concentration of a broad spectrum commercially available insecticide. We then performed chemical and physical measurements on their silks to test whether their mechanical properties, nanostructures and/or amino acid compositions changed as a consequence of exposure to the insecticides. We predicted that the biochemical and neurophysiological stresses induced by insecticide exposure will affect spinning processes and, as a consequence, induce variability in the mechanical properties, nanostructures and amino acid composition of the silk.

2. Material and methods

2.1. Spider collection and pre-treatment

We collected 60 adult female *P. audax* (body mass ≈ 0.1–0.2 g) from the Rivera region, Uruguay. We collected these spiders from elevated forests outside of arable land so they were free from any prior insecticide or pesticide exposure.

To ensure that all spiders used were of approximately equal size we measured each spider's body length to ±0.1 mm, using digital Vernier calipers (Caliper Technologies Corp., Mountain View, CA, USA), and mass to ±0.001 g, using an electronic balance (Ohaus Corp., Pine Brook, NY, USA) upon collection before placing them in 115 mm (wide) x 45 mm (high) plastic circular containers and returning them to the Centro Universitario de Rivera, in Rivera, Uruguay. Here they were individually placed in 60 mm (wide) x 15 mm (high) Petri® dishes and maintained at 25 ± 5° C, 75± 5% relative humidity, and a 12:12 h (L: D) photoperiod for 5 days. During this pre-experimentation phase the spiders were fed one laboratory reared *Tenebrio molitor* (Coleoptera, Tenebrionidae) daily.

2.2. Experiment

Immediately following the pre-experimentation phase all spiders were reweighed to ensure they were of approximately similar mass to that ascertained upon capture. They were then placed in wooden frames (25 cm × 20 cm x 5 cm) with front and back glass barriers, through which we could view the spiders, and randomly allocated into one of two treatment groups: (1) insecticide exposed, or (2) control. The frame dimensions approximated the maximum dimensions of *P. audax* webs in the field (ML, LFG, SJB pers. obs.) so did not inhibit web building. We considered the day that the spiders were moved into the frames as day one of experimentation. The experiment was terminated after day 15 of experimentation, since this is approximately the length of time it takes for nutrients fed to spiders to effectively influence spider silk properties (Townley et al., 2006; Blamires et al., 2014, 2015).

For our experiment we used the commercially available insecticide Geonex (Geonex Commercial Insecticides, Tafirel SA, Uruguay), a broad spectrum insecticide composed of two complementary active ingredients (the neonicotinoid thiamethoxan and the pyrethroid lambda-cyhalothrin). Thiamethoxam is a synthetic organic insecticide that is effective at controlling most sucking and chewing insect pests. It is delivered to a plant by foliar application and ingested by sucking/chewing insects while feeding. Lambda-Cyhalothrin acts in a similar way as thiamethoxam except it targets a broader array of insects. Spiders are likely to imbibe thiamethoxam and lambda-cyhalothrin in nature by consuming affected insects or exposure to aerosols.

We prepared a 1.41 mg l^{-1} (i.e. 5% of the maximum field registered nominal concentration) solution of the insecticide by dilution in analytical grade acetone, as is standard for insecticide exposure experiments. The exposed spiders received 1.0 μl of the solution

placed on their abdomen, using a 5 μl hand micro-applicator (Burkard Scientific, Uxbridge, U.K.), daily throughout the experimentation period. The control spiders received 1.0 μl of the acetone daily. We considered the insecticide concentration used to be sub-lethal to the spiders on the basis that it is sub-lethal to its target insects (Bredeson et al., 2015) and *P. audax* is many orders of magnitude larger. Moreover, we did not find the exposed spiders to experience any more mortality, tremors, paralysis or uncoordinated movements than the control spiders (see below for details of the procedures). The reason we used a sub-lethal concentration was to evaluate the effects of repeated insecticide exposure on spider silk properties.

We removed the spiders from their enclosure every 24 h and examined them (taking < 10 min each time) under a binocular stereoscope to monitor them for mortality, tremors, paralysis, or uncoordinated movements throughout the experiment. These daily examinations were done to ensure no undue trauma was experienced by spiders from any treatment group and it enabled us to be confident that the acetone had no discernible negative effects on the insecticide exposed or control spiders over the timeframe of the experiment. Since insecticides curtail motor co-ordination in spiders and these actions will be manifested as alterations in the form and/or architecture of any webs built (Benamú et al., 2013), we thus recorded whether or not each spider had built a web prior to these examinations. When we found a spider to have built a web we photographed it and used the program Adobe Photoshop to count the number of radial threads and determine whether or not a spiral thread was present. We could not perform classical orb web architectural measurements, such as those of Venner et al. (2001), Blamires (2010), Pasquet et al. (2013), and others, because the insecticide exposed spiders rarely built webs conforming to a stereotypical orb web geometry.

2.3. Silk collection

Upon termination of the experiment we selected and immobilized ten spiders (five each from the control and exposed experimental treatments) by placing them in a petri dish placed on crushed ice for 30 min. We then placed each spider ventral side up on a 150 mm × 100 mm foam platform and immobilized them using non-adhesive tape and pins before carefully pulling a single MAS fiber from their anterior spinnerets using tweezers. The fibers were collected using a mechanical spool spun at a constant speed (1 m min^{-1}) under controlled temperature (~25 °C) and humidity (~50% R.H.) in still air.

2.4. Tensile testing

We collected five threads of silk from each spider from each treatment (n = 50 threads in total) for tensile testing. In this instance we connected a round headframe to the spool and attached a 240 mm long cardboard strip with six 10 mm × 10 mm square holes punched at 10mm intervals into it (supplementary data, Fig. S1(A)). Double sided sticky tape was stuck onto the cardboard between the holes. The headframe was rotated once ensuring the silk traversed all of the holes and adhered to the tape. The strip was then removed from the headframe and a drop of Elmer's glue applied to the position where the silk contacted the tape. We then cut the cardboard strip perpendicular to the silk thread between the holes, leaving six 10 mm × 10 mm frames holding a single thread of silk (supplementary data, Fig. S1(B)) (total n = 300 frames: 5 threads x 6 frames each from 10 spiders).

One frame was used to ascertain the width of the thread to account for the cross-sectional area in the ensuing tensile tests. This was done by taping the frame to a microscope slide and examining and photographing it under 1000× magnification using a polarized light microscope (CKX41, Olympus, Tokyo, Japan) and SPOT Idea 5 Mp digital camera (Spot Imaging Solutions, Sterling Heights, MI, USA). The images were digitized using Spot Basic 4.7 (Spot Imaging Solutions, Sterling Heights, MI, USA) and the width of the thread determined as a mean of 12 measurements made using Image J (NIH, Bethesda, MD, USA). The remaining 250 frame-mounted silk samples (25 each from 5 individuals per treatment) were taken to the Institute for Frontier Materials, Deakin University, Geelong, Australia, and tensile tests performed as follows.

The cardboard frames containing silk fibers were placed within the grips of a T150 (Agilent Technologies, Santa Clara, CA, USA) universal tensile testing machine, the left and right frame borders were cut away, and the silks stretched at a rate of 0.1 mms^{-1} until the fiber ruptured.

Stress (σ) and strain (ε) were calculated using the equations (Blackledge and Hayashi, 2006):

$$\sigma = \frac{F}{A} \tag{1}$$

and

$$\varepsilon = \log e \frac{L}{L_0} \tag{2}$$

where F is the force applied to the specimen measured using the program Nano Suite 1.0 (Agilent Technologies, Santa Clara CA, USA), and A is the cross-sectional area of the thread calculated from the thread diameter assuming a constant thread volume. L is the instantaneous length of the fiber at a given extension value, measured using Nano Suite 1.0, and L_0 is the original gage length of the fiber (10mm).

Stress versus strain curves were then plotted for each silk tested from which we calculated the properties: (1) ultimate strength, or stress at rupture, (2) extensibility, or strain at rupture, (3) toughness; calculated as the area under the stress versus strain curve, and (4) Young's modulus (stiffness); calculated as the slope of the stress-strain curve during its initial elastic phase.

2.5. X-ray scattering analyses

We removed the headframe from the spool after collecting silk for tensile testing and replaced it with a 50 mm long x 20 mm wide stainless steel cylindrical card holder with a 0.5 mm slit at one end into which individual 3 mm × 1 mm steel frames with 0.5 mm × 0.5 mm windows were placed (supplementary data, Fig. S2(A)). We pulled the silk threads of each spider across the frame window and ran the spool for ~2 h ensuring approximately 2000 rounds of silk were wrapped around the frame windows (supplementary data, Fig. S2(B)).

Wide angle X-ray scattering (WAXS) has been effectively used by researchers to examine and compare the size, density, orientation, and distances between various silk nanostructures (Riekel et al., 1999; Riekel and Vollrath, 2001; Jenkins et al., 2013; Blamires et al., 2015). We accordingly used WAXS at the SAXS/WAXS beamline at Australian Synchrotron, Melbourne, Australia, to conduct a suite of nanostructural measurements for each of the ten (5 individuals x 2 treatments: control and exposed) silk samples as follows.

Each frame containing a silk sample was mounted onto a receptacle placed 330mm from the X-ray beam (collimator diameter = 0.5 mm, beam energy = 12keV) source. A digital camera was set up 650mm from the receptacle enabling us to remotely align the beam with the centre of the specimens from outside the

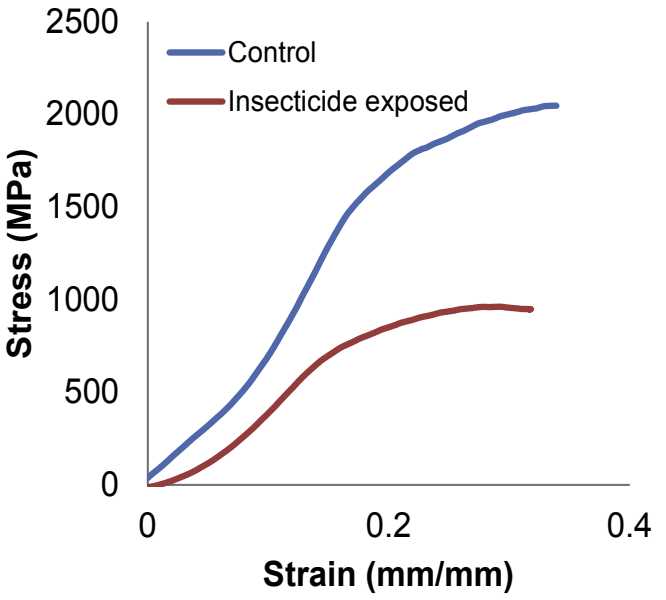

Fig. 1. Example stress versus strain curves for silks of spiders from the insecticide exposed (red curve) and control (blue curve) treatments. (For interpretation of the references to colour in this figure legend, the reader is referred to the web version of this article.)

experimental hutch.

The X-ray scattering was detected for each silk sample by a Mar 165 imaging plate (Q-range = 0.95–1.46 Å). Exposure periods were 10–60 s depending on the density of the sample. Two-dimensional scattering profiles were developed using the program Scatterbrain 2.82 (Australian Synchrotron, Melbourne, Australia). We additionally used Scatterbrain 2.82 to calculate the scattering angles (θ), intensity peaks (I_x), and full width and half width maximum intensities (FWHM) at the (0 2 0) and (2 1 0) Bragg scattering peaks, the peaks considered to be associated with scattering from crystalline β–sheets in silk (Riekel et al., 1999), and the amorphous halo from the profiles. We subsequently used these parameters to derive, and compare across treatments:

(i) The length scale, d, an estimate of the length over which crystalline order persists (Frischetti et al., 2004), calculated using the equation:

$$d = \frac{n\lambda}{\sin\theta} \quad (3)$$

where n is an arbitrary positive integer and λ is the wavelength of the incident X-ray (i.e. 1.032 Å), and θ is the scattering angles of the (0 2 0) and (2 1 0) scattering peaks.

(ii) Mean crystal size, τ, calculated using the Debye-Scherrer's equation (Riekel et al., 1999):

$$\tau = \frac{K\lambda}{\beta\cos\theta} \quad (4)$$

where K is the shape factor, which we assumed to be derived from a sphere, hence a value of 0.9 (Glisovic et al., 2008), and β is full line widths at half the maximum intensity after accounting for instrumental broadening.

(iii) Relative crystalline intensity, I_{020}/I_{210}, with I_{020} and I_{210} representing the sum of the intensity peaks at the (0 2 0) and (2 1 0) reflection peaks respectively (Plaza et al., 2012).
(iv) The crystallinity index, *Xc*, calculated according to Grubb and Jelinski (1997), and
(v) Herman's orientation function, f_c, calculated using the equation (Jenkins et al., 2013):

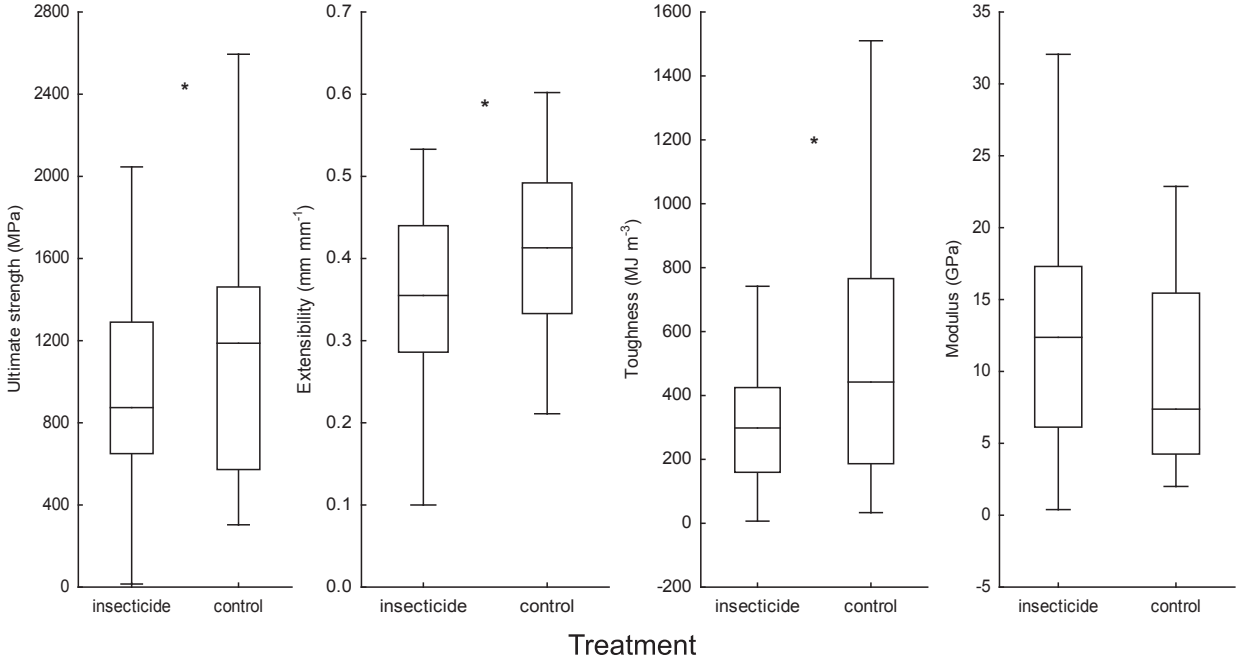

Fig. 2. Box-Whisker plots comparing the mechanical properties ultimate strength, extensibility, toughness, and stiffness (modulus) between insecticide exposed (insecticide) and control treatments. Boxes display the median, 25% and 75% quartiles, and range excluding outliers.

$$fc = \frac{(3\{\cos 2\phi\} - 1)}{2} \quad (5)$$

where φ is the angle between the c axis and the fiber axis, $\{\cos^2\varphi\}$ is the azimuthal width of the equatorial reflections at (0 2 0) and (2 1 0) determined using the equation (Grubb and Jelinski, 1997):

$$\{\cos 2\varphi\} = 1 - A\{\cos 2\varphi 1\} - B\{\cos 2\varphi 2\} \quad (6)$$

where A = 0.8 and B = 1.2.

2.6. Amino acid composition analysis

Upon completion of the WAXS experiments we removed the silk samples from their frames and weighed them to the nearest 0.001 mg on an electronic balance (Pioneer PA214C, Ohaus, Pine Brook NJ, USA). The silk was then placed in 1 ml Eppendorf tubes and sent to the Australian Protemic Analysis Facility, Sydney, Australia, where mole percentages of the amino acids glutamine, serine, proline, glycine, and alanine (since these represent at least 90% of the total amino acids in the MAS of most spiders; Work and

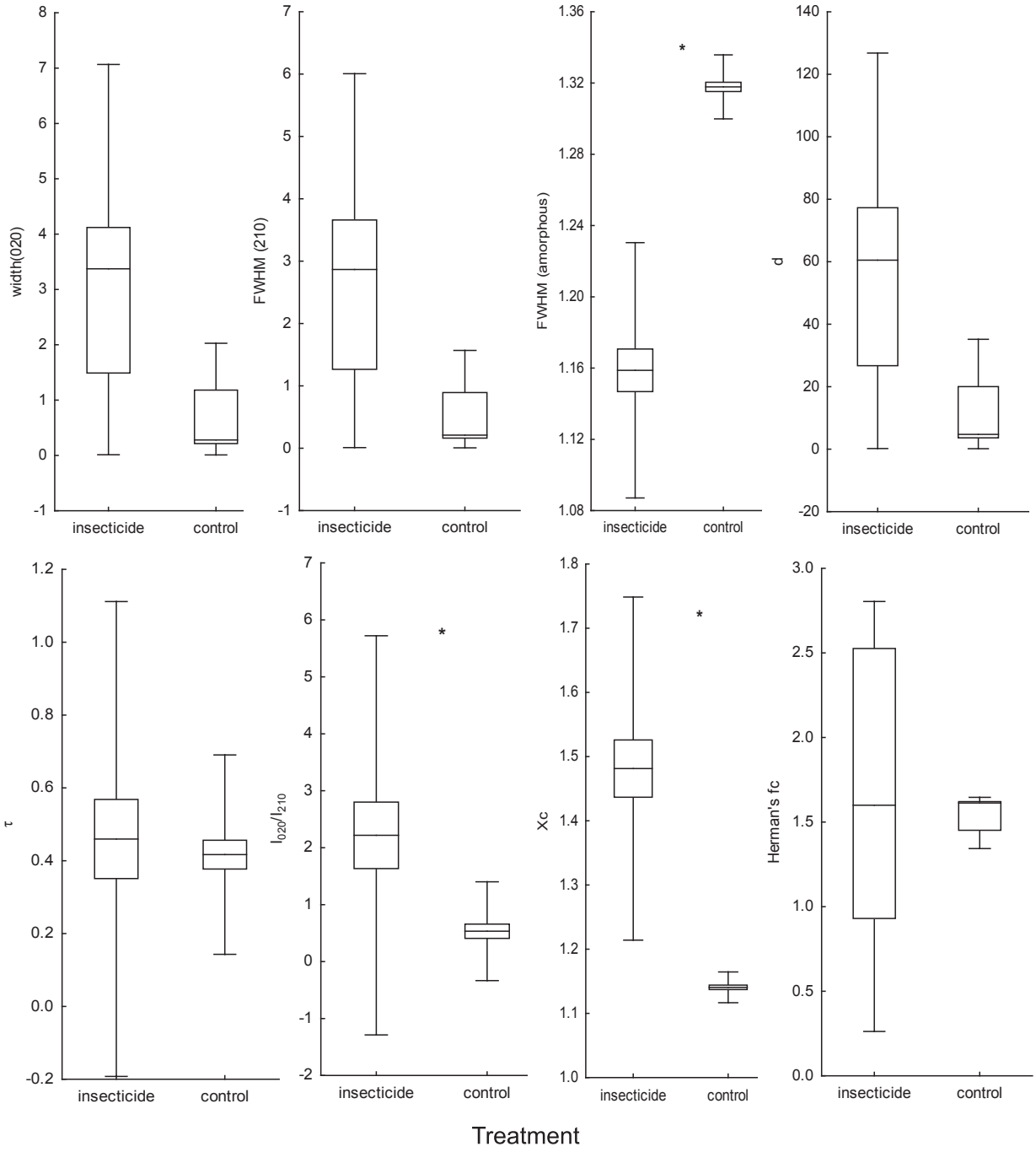

Fig. 3. Box-Whisker plots comparing the nanostructural parameters FWHM for the (0 2 0) diffraction peak, FWHM for the (2 1 0) diffraction peak (these are estimates of crystalline alignment at the (0 2 0) and (2 1 0) Bragg diffraction peaks respectively), FWHM for the amorphous halo (an estimate of the amorphous region alignment), length scale, d, mean crystal size (Å), τ, relative crystalline intensity, I_{020}/I_{210}, crystallinity index, X_c, and Herman's crystalline orientation function, f_c, between insecticide exposed (insecticide) and control treatments. Boxes display the median, 25% and 75% quartiles, and range excluding outliers.

Table 1
Results of a sum-of-squares of the whole model (SS Whole model) *vs* sum-of-squares of the residuals (SS Residuals) analysis derived for a Multivariate analyses of variance (MANOVA) comparing *P. audax* silk nanostructures (FWHM for the (0 2 0) and (2 1 0) diffraction peaks and amorphous halo, d, τ, I_{020}/I_{210}, X_c and f_c) from the insecticide and control treatments.

Dependent variable	Multiple R^2	Adjusted R^2	df model	df residual	F	*p*
FWHM (0 2 0)	0.0917	0.0439	1	19	1.9191	0.1820
FWHM (2 1 0)	0.1202	0.0739	1	19	2.5963	0.1326
FWHM (amorphous)	0.9210	0.9169	1	19	221.7736	<0.0001[a]
d	0.1069	0.0599	1	19	2.2750	0.1479
τ	0.0888	−0.0432	1	19	0.9703	0.3369
I_{020}/I_{210}	0.9196	0.1490	1	19	4.5042	0.0471[a]
X_c	0.8052	0.7950	1	19	78.5767	<0.0001[a]
Herman's f_c	0.0485	−0.0014	1	19	0.1701	0.6847

[a] Indicates an across treatment significant difference.

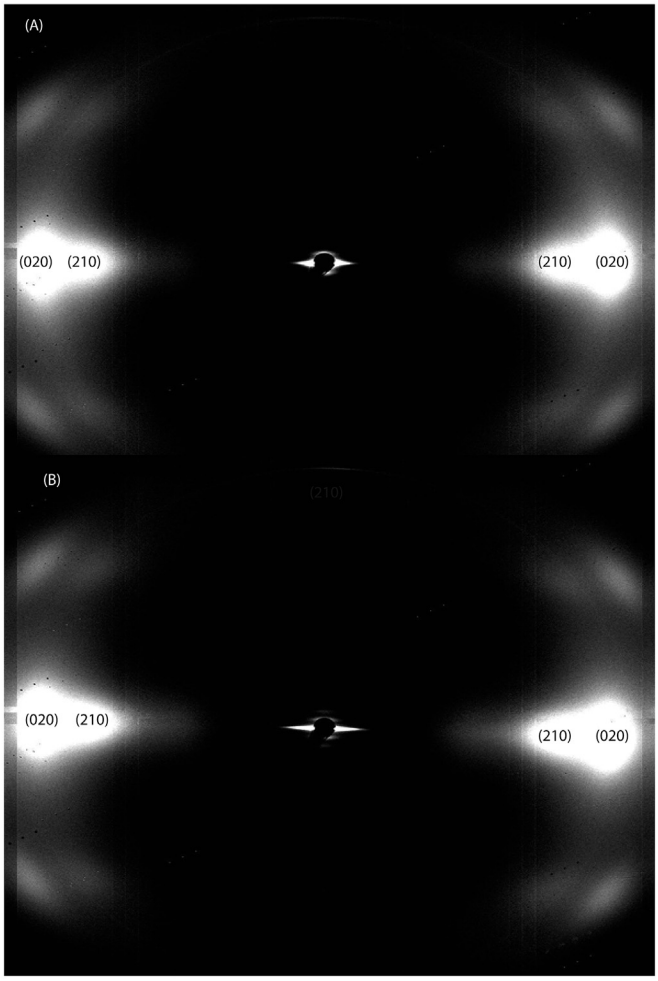

Fig. 4. Examples of the two-dimensional WAXS images from the MA silk of: (A) insecticide exposed and (B) control treatment spiders. The brightest (whitest) regions represent the (0 2 0) and (2 1 0) Bragg diffraction peaks as indicated on the images. The light outer ring represents the 'amorphous halo'.

Young, 1987) were determined using High Performance Liquid Chromatography (Schuster, 1988).

2.7. Statistical analyses

We compared the mechanical properties: ultimate strength, extensibility, toughness and stiffness between the treatments by a generalized linear mixed model using the R packages car (Fox and Weisberg, 2011) and lme4 (Bates et al., 2015). We assigned each mechanical property as a response variable. The two treatments were explanatory variables, and silk diameters the covariate. Since we replicated the analyses for individual spiders, we included the individual spider number as a random effect in the model. We reported the results as Wald chi-squared with corresponding p-values. We compared the crystalline and non-crystalline nanostructures (i.e. the parameters: FWHM at the (0 2 0) and (2 1 0) scattering peaks and amorphous halo, d, τ, I_{020}/I_{210}, X_c and f_c) and mole compositions of glutamine, serine, proline, glycine, and alanine compositions between treatments using multivariate analyses of variance (MANOVAs) followed by Fisher's Post-hoc analyses to identify the influential variables. Prior to analyses we checked for heterogeneity of variances using a Levene's tests and $\log_{10}$ transformed data that failed the test. Analyses were performed using the programs R 3.3.1 (R Core Team, 2016) and STATISTICA 13.0 (Dell Software, Tulsa OK, USA) with an R program extension.

3. Results and discussion

Within the first 24 h of experimentation the control spiders had all built webs, while no insecticide exposed spiders built webs. Spiders in the insecticide exposed treatment took around 48 h longer to construct a web (supplementary data, Fig. S3). By termination of the experiment only 16 of 30 (53%) insecticide exposed spiders had built webs. The insecticide exposed spiders build irregular webs that lacked spiral threads (supplementary data, Fig. S4). Similar web architectural impairments have been reported for other web building spiders exposed to insecticides (Benamú et al., 2007, 2013; Pekar, 2013; Pasquet et al., 2016). We thus conclude that the insecticide dose used here adversely affected the spider's motor co-ordination, thus their ability to construct an orb web. Production of the sticky spiral capture threads may have also been impaired.

The stress versus strain curves for the silks of the insecticide exposed spiders visually differed from those of the control treatment spiders (Fig. 1). Our subsequent analyses found the mechanical properties of the silks from spiders receiving insecticide exposure differed to those of spiders not receiving exposure (i.e. the controls); with stronger (Wald $\chi^2_1 = 5.59$, $p = 0.01$), more extensible (Wald $\chi^2_1 = 4.47$, $p = 0.03$) and tougher (Wald $\chi^2_1 = 7.02$, $p < 0.001$) silks produced by spiders from the control treatment (Fig. 2).

The two-dimensional X-ray scattering profiles for the insecticide exposed spiders' silks and control treatment spiders' silks are shown in Fig. 3(A) and (B) respectively. The nanostructures of the silks from spiders receiving the insecticide and control treatments differed (MANOVA, Intercept: Wilks $\lambda_{9,11} < 0.001$, $p < 0.001$, Treatment: Wilks $\lambda_{9,11} = 0.003$, $p < 0.001$). The relative crystalline intensity (I_{020}/I_{210}) and crystallinity index (X_c) were greater in the silks of insecticide treated spiders, and FWHM at the amorphous

Table 2
Results of a sum-of-squares of the whole model (SS Whole model) *vs* sum-of-squares of the residuals (SS Residuals) analysis derived for a Multivariate analyses of variance (MANOVA) comparing the silk amino acid (% gly = glycine composition, and % ala = alanine composition, % pro = proline composition, % glu = glutamine composition, % ser = serine composition) mole compositions for *Parawixia audax* from the insecticide and control treatments.

Dependent variable	Multiple R^2	Adjusted R^2	df model	df residual	F	*p*
% gly	0.2948	0.1942	1	8	4.9360	0.0210[a]
% ala	0.2253	0.1590	1	8	4.463	0.0315[a]
% pro	0.2931	0.1922	1	8	4.631	0.0239[a]
% glu	0.1625	0.0579	1	8	4.5532	0.0369[a]
% ser	0.0217	0.1244	1	8	5.2790	0.1690

[a] Indicates an across treatment significant difference.

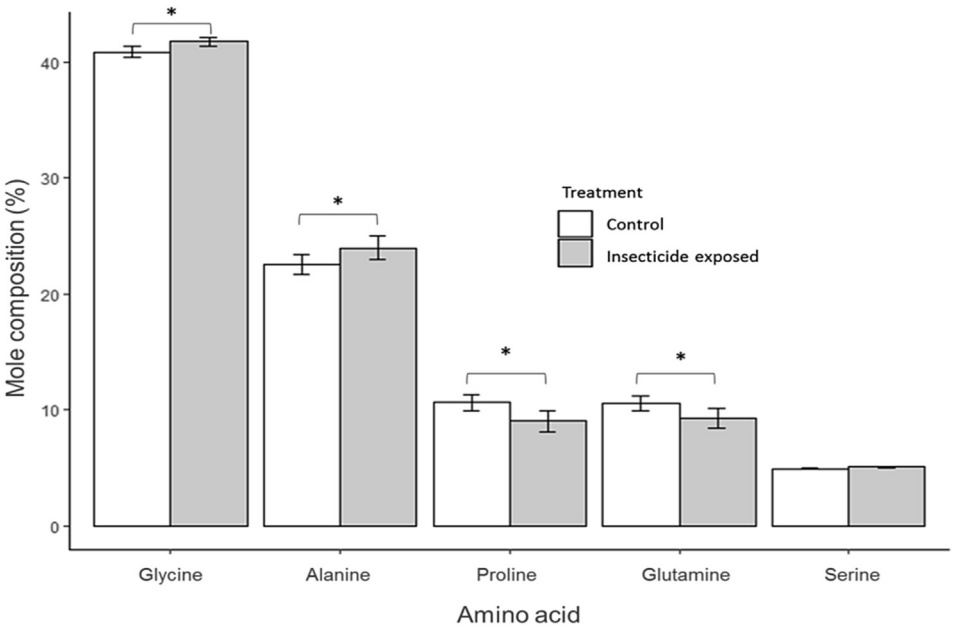

Fig. 5. Between treatment (control versus insecticide exposed) comparison of the mole compositions of the amino acids glycine, alanine, proline, glutamine serine between insecticide exposed (insecticide) and control treatments. Error bars show ±1 s. e.

halo was greater in the silks of the control spiders (Table 1, Fig. 4). These results led us to conclude that crystallinity and crystalline intensity were greater in the insecticide treated spider's silks, while alignment in the amorphous region nanostructures was greater in the control treatment spider's silks. The difference in nanostructural alignment likely explains the mechanical property differences across treatments. Indeed models, simulations and experiments all show that variation in structure and alignment within the highly mobile amorphous region enhances MAS strength and extensibility (Sponner et al., 2007; Keten et al., 2010; Blamires et al., 2015). Our mechanical property analyses confirmed those predictions.

The amino acid mole compositions in the silks of spiders receiving the insecticide treatment differed from those receiving the control treatment (MANOVA, Intercept: Wilks $\lambda_{5,4} < 0.001$, $p < 0.001$, Treatment: Wilks $\lambda_{5,4} = 0.407$, $p < 0.045$). We found that silks of the control treatment spiders contained relatively more proline and glutamine, but less alanine and glycine than the silks of spiders in the control treatment (Table 2, Fig. 5). Such compositional differences across treatments are suggestive of differential expressions of the two MAS proteins (spidroins), MaSp1 and MaSp2 (Xu and Lewis, 1990; Hinman and Lewis, 1992; Craig et al., 1999; Blamires et al., 2012). Explicitly, the silks of the control spiders appeared to contain more MaSp2 (identified by their greater proline and glutamine composition), while the insecticide exposed spider's silk appeared to contain more MaSp1.

MaSp1 consists of multiple poly-glycine, glycine-alanine or poly-alanine repeating sequences, which promotes the formation of crystalline β−sheet nanostructures in the assembled silk fibers (Xu and Lewis, 1990). These structures usually bestow MAS with strength and stiffness (Hayashi et al., 1999; Vollrath et al., 2013; Blamires et al., 2017). Our WAXS analyses found greater crystallinity, hence a greater proportion of β−sheets relative to other nanostructures (Jenkins et al., 2013), in the MAS of insecticide exposed spiders. We can ascribe our finding as indicative of a greater proportion of MaSp1 in these silks.

MaSp2, on the other hand, consists of sequences containing glycine, alanine, glutamine and proline, which promote the formation of β-spirals and type-II β-turns in the amorphous region (Hinman and Lewis, 1992) and bestow the silk with greater extensibility (Hayashi et al., 1999; Blamires et al., 2017). The greater nanostructural alignment in the amorphous region in the silks of control treatment spiders thus appears to be a consequence of greater MaSp2 expression (Hayashi et al., 1999). The greater strength and extensibility found in the silks of the control spiders compared to the insecticide exposed spiders was nevertheless surprising as the greater proportion of β-spirals and β-turn nanostructures in the MaSp2 predominant silks of the control spiders should have endowed them with greater extensibility but inferior strength. We found, however, greater amorphous region alignment (indicated by our WAXS analyses as greater FWHM at the amorphous halo) as well as increased crystalline region densities in the

silks of the control treatment spiders and these nanostructural arrangements are known to simultaneously promote silk strength and extensibility (Keten et al., 2010). Covariation in nanostructures probably occurs because the proline-containing sequences in MaSp2 promote hydrogen bonding in the amorphous region inducing it to align strongly along the fiber axis (Vollrath et al., 2013), resulting in greater fiber extensibility and toughness when under strain (Keten et al., 2010; Plaza et al., 2012; Blamires et al., 2016). Hence we conclude that the differences in MAS amino acid compositions between treatments indicates differential expression of MaSp1 and MaSp2, which explains the across treatment differences in silk nanostructures and mechanical properties.

The quandary for us to now ponder is the mechanism by which insecticide exposure might induce MaSp expression variation in the MAS of *P. audax*. We note that similar shifts in spidroin expressions and MAS properties have been shown for spiders under nutritional stress (Blamires et al., 2012, 2015). Furthermore, there is speculation that these expression shifts occur because MaSp2 is metabolically more costly to synthesize than MaSp1 so is downregulated by spiders when under metabolic stress (Craig et al., 1999; Blamires et al., 2012). Insecticides such as thiamethoxan and lambda-cyhalothrin disrupt nicotinic acetylcholine receptor proteins to inhibit neural propagation in invertebrates (Tomizawa et al., 1995; Jones and Sattelle, 2010). Even at sub-lethal concentrations these actions can induce moderate to severe metabolic stress (Oliveira et al., 2014). Perhaps a change in the metabolic output in the insecticide exposed spiders necessitated a reduction in MaSp2 expression in their MAS. Aggregate silk, which forms part of the sticky spiral capture threads of orb webs, has also been implicated as coming at a substantial metabolic cost (Townley et al., 2006; Blamires et al., 2014, 2017). Insecticide-induced metabolic stress, accordingly, might also explain the lack of spiral threads in the webs of the insecticide exposed spiders.

4. Conclusions

We exposed the orb web spider *Parawixia audax* to a broad spectrum insecticide, which resulted in impairments in the nanostructural and mechanical properties of their major ampullate silks. The silks of the control spiders were stronger, tougher and more extensible than that of the spiders exposed to insecticides. Examination of the silk nanostructures using WAXS found that crystallinity and crystal intensities were greater in the silks of the insecticide exposed spiders than those of the control spiders, while amorphous nanostructural alignment was greater in the control spider's silks. Spiders receiving insecticides produced silks with greater proline and glutamine compositions, indicative of an enhancement in the expression of the silk protein MaSp2. The control spider's silks, however, had greater serine, glycine, and alanine compositions, indicative of greater MaSp1 expression. It thus seems likely that MaSp2 was downregulated in the insecticide exposed spider's silks, which led to the nanostructural and mechanical property changes. The resultant impairment in silk properties, coupled with the severely negative influence on web building, means that insecticide exposure most likely reduces the spider's prey catching capabilities. We recommend more experiments be performed to fully understand the indirect lethal and non-lethal impacts of insecticide use on other non-target invertebrates.

Acknowledgements

Our research was supported by an Australian Research Council (Discovery Early Career Researcher Award DE140101281) to S.J.B. Adrian Hawley, Australian Synchrotron, assisted with WAXS experiments and analyses. Ben Allardyce, Hamish Craig and Jonas Wolff assisted with silk tensile testing. Juan Sebastian Garcia, Carmen Viera and Enrique Castiglioni provided logistical support. Jordi Moya-Laraño made suggestions on statistical analyses.

Appendix A. Supplementary data

Supplementary data related to this article can be found at http://dx.doi.org/10.1016/j.chemosphere.2017.04.079.

References

Andersson, M., Holm, L., Ridderstrale, Y., Johansson, J., Rising, A., 2013. Morphology and composition of the spider major ampullate gland and dragline silk. Biomacromolecules 14, 2945–2952.
Asquith, D., Hull, L.A., 1973. *Stethorus punctum* and pest population responses to pesticide treatments on apple trees. J. Econom. Entomol. 66, 1197–2103.
Bates, D., Maechler, M., Bolker, B., Walker, S., 2015. Fitting linear mixed-effects models using lme4. J. Stat. Softw. 67, 1–48.
Benamú, M.A., 1999. Estudio preliminar de la araneofauna presente en mandarina cultivada en Vitarte, Lima. Perú. Rev. Per. Ent. 41, 154–157.
Benamú, M.A., 2010. Composición y estructura de la comunidad de arañas en el sistema de cultivo de soja transgénica. Doctoral Dissertation. Universidad Nacional de La Plata, Facultad de Ciencias Naturales y Museo, La Plata, Argentina.
Benamú, M.A., Schneider, M.A., Gonzalez, A., Sanchez, N.E., 2013. Short and long-term effects of three neurotoxic pesticides on biological and behavioural attributes of the orb-web spider *Alpaida veniliae* (Araneae, Araneidae): implications for IPM programs. Ecotxicology 22, 1155–1164.
Benamú, M.A., Schneider, M.A., Pineda, S., Sánchez, N., González, A., 2007. Sublethal effects of two neurotoxican insecticides on *Araneus pratensis* (Araneae: Araneidae). Comm. Appl. Biol. Sci. 72, 557–559. Ghent University.
Blackledge, T.A., Hayashi, C.Y., 2006. Silken toolkits: biomechanics of silk fibers spun by the orb web spider *Argiope arentata* (Fabricius 1775). J. Exp. Biol. 209, 2452–2461.
Blamires, S.J., 2010. Plasticity in extended phenotypes: orb web architectural responses to variations in prey parameters. J. Exp. Biol. 213, 3207–3212.
Blamires, S.J., Blackledge, T.A., Tso, I.M., 2017. Physico-chemical property variation in spider silks: ecology, evolution and synthetic production. Ann. Rev. Entomol. 62, 443–460.
Blamires, S.J., Kasumovic, M.M., Tso, I.M., Martens, P.J., Hook, J.M., Rawal, A., 2016. Decoupling of spidroin expression and protein structure in spider dragline silks. Int. J. Mol. Sci. 17, 1294.
Blamires, S.J., Liao, C.P., Chang, C.K., Chuang, Y.C., Wu, C.L., Blackledge, T.A., Sheu, H.S., Tso, I.M., 2015. Mechanical performance of spider silk is robust to nutrient-mediated changes in protein composition. Biomacromolecules 16, 1218–1225.
Blamires, S.J., Sahni, V., Dhinojwala, A., Blackledge, T.A., Tso, I.M., 2014. Nutrient deprivation induces property variations in spider gluey silk. PLoS One 9, e88487.
Blamires, S.J., Wu, C.L., Tso, I.M., 2012. Variations in protein intake induces variations in spider silk expression. PLoS One 7, e31626.
Bredeson, M.M., Reese, R.N., Lungren, J.G., 2015. The effects of insecticide dose and herbivore density on tri-trophic effects of thiamethoxam in a system involving wheat, aphids, and ladybeetles. Crop Prot. 69, 70–76.
Breslauer, D.N., Kaplan, D.L., 2012. Silks. In: Tirrell, D.A., Langer, R. (Eds.), Polymer Science: a Comprehensive Reference Volume 9: Polymers in Biology and Medicine. Elsevier, Amsterdam, The Netherlands, pp. 57–69.
Craig, C.L., Hsu, M., Kaplan, D.L., Pierce, M.E., 1999. A comparison of the composition of silk proteins produced by spiders and insects. Int. J. Biol. Macromol. 24, 109–118.
Craig, C.L., Riekel, C., Herberstein, M.E., Weber, R.S., Kaplan, D.L., Pierce, M.E., 2000. Evidence for diet effects on the composition of silk proteins produced by spiders. Mol. Biol. Evol. 17, 1904–1913.
Dai, Y., Zhao, Y., Zhang, W., Yu, C., Ji, W., Xu, W., Ni, J., Yuan, S., 2010. Biotransformation of thianicotinyl neonicotinoid insecticides: diverse molecular substituents response to metabolism by bacterium *Stenotrophomonas maltophilia* CGMCC 1.1788. Bioresour. Technol. 101, 3838–3843.
Desneux, N., Decourtye, A., Delpuech, J., 2007. The sublethal effects of pesticides on beneficial arthropods. Ann. Rev. Entomol. 52, 81–106.
Elbert, A., Haas, M., Springer, B., Thielert, W., Nauen, R., 2008. Applied aspects of neonicotinoid uses in crop protection. Pest Manag. Sci. 64, 1099–1105.
Fox, J., Weisberg, S., 2011. An R Companion to Applied Regression, second ed. Sage, Thousand Oaks CA, USA.
Frischetti, R.F., Rodi, D.J., Gore, D.B., Makowski, L., 2004. Wide-angle X-ray solution scattering as a probe of ligand-induced conformational changes in proteins. Chem. Biol. 11, 1431–1441.
Glisovic, A., Vehoff, T., Davies, R.J., Salditt, T., 2008. Strain dependent structural changes of spider dragline silk. Macromolecules 41, 390–398.
Grubb, D.T., Jelinski, L.W., 1997. Fiber morphology of spider silk: the effects of tensile deformation. Macromolecules 30, 2860–2867.

Hagn, F., Thamm, C., Scheibel, T., Kessler, A., 2011. pH-dependent dimerization and salt-dependent stabilization of the N-terminal domain of spider dragline silk—implications for fiber formation. Angew. Chem. Int. Ed. 50, 310–313.
Hayashi, C.Y., Shipley, N.H., Lewis, R.V., 1999. Hypotheses that correlate the sequence, structure, and mechanical properties of spider silk proteins. Int. J. Biol. Macromol. 24, 271–275.
Heim, M., Keerl, D., Scheibel, T., 2009. Spider silk: from soluble protein to extraordinary fiber. Angew. Chem. Int. Ed. 48, 3584–3596.
Heim, M., Romer, L., Scheibel, T., 2010. Hierarchical structures made of proteins. The complex architecture of spider webs and their constituent silk proteins. Chem. Soc. Rev. 39, 156–164.
Hinman, M.B., Lewis, R.V., 1992. Isolation of a clone encoding a second dragline silk fibroin: *Nephila clavipes* dragline silk is a two-protein fiber. J. Biol. Chem. 267, 19320–19324.
Hoefler, C., Chen, A., Jakob, E., 2006. The potential of a jumping spider, *Phidippus clarus*, as a biocontrol agent. J. Econ. Entomol. 99, 432–436.
Honda, H., Tomizawa, M., Casida, J.E., 2006. Neonicotinoid metabolic activation and inactivation established with coupled nicotinic receptor-CYP3A4 and -aldehyde oxidase systems. Toxicol. Lett. 161, 108–114.
Ishaaya, I., Barazani, A., Kontsedalov, S., Horomitz, A.R., 2007. Insecticides with novel modes of action: mechanisms, selectivity and cross-resistance. Entomol. Res. 37, 148–152.
Jelinski, L.W., 1998. Establishing the relationship between structure and mechanical function in silks. Curr. Opin. Sol. Stat. Mater. Sci. 3, 237–245.
Jenkins, J.E., Sampath, S., Butler, E., Kim, J., Henning, R.W., Holland, G.P., Yarger, J.L., 2013. Characterizing the secondary protein structure of black widow dragline silk using solid-state NMR and X-ray diffraction. Biomacromolecules 14, 3472–3483.
Jones, A.K., Sattelle, D.B., 2010. Diversity of insect nicotinic acetylcholine receptor subunits. In: Thany, S.H. (Ed.), Insect Nicotinic Acetylcholine Receptors. Landes Bioscience and Springer Science, Berlin, pp. 25–43.
Keten, S., Xu, Z., Ihle, M., Buehler, M.J., 2010. Nanoconfinement controls stiffness, strength and mechanical toughness of β-sheet crystals in silk. Nat. Mater. 9, 359–367.
Lacava, M., 2014. Versatilidad predadora de las arañas lobo (Araneae, Lycosidae) y su efecto sobre insectos de importancia económica en soja. MSc dissertation. Universidad de la República, Facultad de Ciencias, Montevideo, Uruguay.
Landis, D.A., Wratten, S.D., Gurr, G.M., 2000. Habitat management to conserve natural enemies of arthropod pests in agriculture. Ann. Rev. Entomol. 45, 175–201.
Ministerio de Ganaderia Agricultura y pesca, 2013. Anuario estadistico agropecuario, p. 270.
Michalko, R., Kosulic, O., 2016. Temperature-dependent effects of two neurotoxic insecticides on predatory potential of *Philodromus* spiders. J. Pest Sci. 89, 517–527.
Öberg, S., Ekbom, B., Bommarco, R., 2007. Influence of habitat type and surrounding landscape on spider diversity in Swedish agroecosystems. Agr. Ecosyst. Environ. 122, 211–219.
Oliveira, R.A., Roat, T.C., Carvalho, S.M., Malispina, O., 2014. Side-effects of thiamethoxam on the brain and midgut of the African honeybee *Apis mellifer* (Hymenoptera: Apidae). Env. Toxicol. 29, 1122–1133.
Papadopoulos, P., Solter, J., Kremer, F., 2009. Hierarchies in the structural organization of spider silk—a quantitative model. Coll. Polym. Sci. 287, 231–236.
Pasquet, A., Marchal, J., Anotaux, M., Leborgne, R., 2013. Imperfections in a perfect architecture: the orb web of spiders. Eur. J. Entomol. 110, 493–500.
Pasquet, A., Tupinier, N., Mazzia, C., Capowiez, Y., 2016. Exposure to spinosad affects orb-web spider (*Agalenatea redii*) survival, web construction and prey capture under laboratory conditions. J. Pest Sci. 89, 507–515.
Pekar, S., 2013. Side effects of synthetic pesticides on spiders. In: Nentwig, W. (Ed.), Spider Ecophysiology. Springer, Berlin, Germany, pp. 415–427.
Pisa, L.W., Amaral-Rogers, V., Belzunces, L.P., Bonmatin, J.M., Downs, C.A., Goulson, D., Kreutzweiser, D.P., Krupke, C., Liess, M., McField, M., Morrissey, C.A., Noome, D.A., Settele, J., Simon-Delso, N., Stark, J.D., Van der Sluijs, J.P., Van Dyck, H., Wiemers, M., 2015. Effect of neonicotinoids and fipronil on non-target invertebrates. Env. Sci. Poll. Bull. 22, 68–102.
Plaza, G.R., Perez-Rigueiro, J., Riekel, C., Perea, G.B., Agullo-Rueda, F., Burghammer, M., Guinea, G.V., Elices, M., 2012. Relationship between microstructure and mechanical properties in spider silk fibers: identification of two regimes in the microstructural changes. Soft Matter 8, 6015–6026.
R Core Team, 2016. R: a Language and Environment for Statistical Computing. R Foundation for Statistical Computing, Vienna, Austria.
Riekel, C., Branden, C.I., Craig, C.L., Ferrero, C., Heidelbach, F., Muller, M., 1999. Aspects of X-ray diffraction on single spider fibers. Int. J. Biol. Macromol. 24, 179–186.
Riekel, C., Vollrath, F., 2001. Spider silk fibre extrusion: combined wide- and small-angle X-ray microdiffraction experiments. Int. J. Biol. Macromol. 29, 203–210.
Rising, A., Johansson, J., 2015. Toward spinning artificial spider silk. Nat. Chem. Biol. 11, 309–315.
Royaute, R., Buddle, C.M., Vincent, C., 2015. Under the influence: sublethal exposure to an pesticide affects personality expression in a jumping spider. Funct. Ecol. 29, 262–270.
Schuster, R., 1988. Determination of amino acids in biological, pharmaceutical, plant and food samples by automated precolumn derivitatization and high-performance liquid chromatography. J. Chromatogr. 431, 271–284.
Schwarze, S., Zwettler, F.U., Johnson, C.M., Neuweiler, H., 2013. The N-terminal domains of spider silk proteins assemble ultrafast and protected from charge screening. Nat. Comm. 4, 2815.
Sponner, A., Vater, W., Monajembashi, S., Unger, E., Grosse, F., Weissart, K., 2007. Composition and hierachical organisation of a spider silk. PLoS One 3, e998.
Sunderland, K., 1999. Mechanisms underlying the effects of spiders on pest populations. J. Arachnol. 27, 308–316.
Symondson, W.O.C., Sunderland, K.D., Greenstone, M.H., 2002. Can generalist predators be effective biocontrol agents? Ann. Rev. Entomol. 47, 561–594.
Tso, I.M., Wu, H.C., Hwang, I.R., 2005. Giant wood spider *Nephila pilipes* alters silk protein in response to prey variation. J. Exp. Biol. 208, 1053–1061.
Tomizawa, M., Casida, J.E., 2005. Neonicotinoid insecticide toxicology: mechanisms of selective action. Ann. Rev. Pharmacol. Toxicol. 45, 247–268.
Tomizawa, M., Otsuka, H., Miyamoto, T., Yamamoto, I., 1995. Pharmacological effects of imidacloprid and its related compounds on the nicotinic acetylcholine receptor with its ion channel from the Torpedo electric organ. J. Pest. Sci. 20, 49–56.
Townley, M.A., Tllinghast, E.K., Neefus, C.D., 2006. Changes in composition of spider orb web sticky droplets with starvation and web removal and synthesis of sticky droplet compounds. J. Exp. Biol. 209, 1463–1486.
Venner, S., Thevenard, L., Pasquet, A., Leborgne, R., 2001. Estimation of the web's capture thread length in orb-weaving spiders: determining the most efficient formula. Ann. Entomol. Soc. Am. 94, 490–496.
Vollrath, F., Porter, D., Holland, C., 2013. The science of silks. MRS Bull. 38, 73–80.
Work, R.W., Young, T.C., 1987. The amino acid compositions of major ampullate and minor ampullate silks of certain orb-web building spiders (Araneae, Araneidae). J. Arachnol. 15, 65–80.
Xu, M., Lewis, R.V., 1990. Structure of a protein superfiber: spider dragline silk. Proc. Nat. Acad. Sci. U. S. A. 87, 7120–7124.